SLAC-PUB-16507

Minimization of Betatron Oscillations of Beam Injected into a Time-Varying Lattice

Alexander Scheinker*
Los Alamos National Laboratory

Xiaobiao Huang† and Juhao Wu
SLAC National Accelerator Laboratory

(Dated: April 12, 2016)

We report on a beam-based experiment performed at the SPEAR3 storage ring of the Stanford Synchrotron Radiation Lightsource (SSRL) at SLAC National Accelerator Laboratory, in which a model-independent optimization algorithm was utilized to minimize betatron oscillations in the presence of a time-varying kicker magnetic field, by automatically tuning the pulse width, voltage, and delay of two other kicker magnets, and the current of two skew quadrupole magnets, simultaneously, in order to optimize injection kick matching. Adaptive tuning was performed on all 8 parameters simultaneously based only on minimization of a measure of betatron oscillation magnitudes over 256 turns. The scheme was able to quickly re-tune the lattice to minimize oscillations after a magnet settings step change, as well as able to continuously retune the lattice while the field strength of the third kicker was continuously, quickly varied ($\pm 6\%$ sinusoidal voltage change over 1.5 hours). The results of this work are a particular in-hardware demonstration of the adaptive scheme's ability to model-independently tune many coupled components simultaneously, which may be useful for uncertain systems, especially time-varying parameters which require repeated re-tuning.

PACS numbers: 41.85.Lc, 02.30.Yy, 29.20.-c, 02.60.-x

I. INTRODUCTION

Particle accelerators are large, complex systems, with nonlinear coupling between many components, and time-varying, uncertain disturbances, including magnet power source fluctuations, thermal cycling of various components, magnet position and alignment perturbations during construction/maintenance, and hysteresis, to name a few. For the problem of tuning many coupled components which have a deterministic effect on the particle beam, there exist a large family of optimization schemes which take place offline, during the design stage [1].

Genetic algorithms (GA) and multi-objective genetic algorithms (MOGA) have been very successful for the design and optimization of radio frequency cavities [2], photoinjectors [3], damping rings [4], storage ring dynamics [5], lattice design [6], neutrino factory design [7], simultaneous optimization of beam emittance and dynamic aperture [8], free electron laser linac drivers [9] and various other accelerator physics applications [10]. Furthermore, multi-objective particle swarm optimization (MOPSO), an extension of MOGA, has recently been demonstrated for emittance reduction, with convergence rates exceeding those of MOGA approaches [11]. Genetic algorithms are able to search over a large parameter space and result in global optimization, however, model-based results are optimal only relative to a known model. In most cases, once the machine is actually built, further tweaking is required due to imperfect models and finite precision of construction. Recently, the GA method has been demonstrated on-line, on an actual accelerator rather than based on a model, successfully minimizing the vertical beam size of the SPEAR3 storage ring [12]. Another optimization method is Robust conjugate direction search (RCDS), a local (may be trapped in local minima) model-independent algorithm which is able to optimization many parameter systems with fast convergence rates and is able to handle noisy systems [13, 14]. RCDS and particle swarm have also been used for online optimization of nonlinear storage ring dynamics [15].

Both the GA and RCDS approaches are best suited for time-invariant systems, an RCDS method for dealing with slowly drifting systems is under consideration, but further development is needed. In this work, we utilize a local, model-independent extremum seeking (ES) algorithm, whose convergence can also suffer due to local minima, but whose simplicity and speed of convergence allows for real time tracking of a many parameter time-varying nonlinear system. The ES algorithm utilized in this work is a recently developed general approach for the stabilization of noisy, uncertain, open-loop unstable, time-varying systems [16, 17]. This method has been implemented in simulation to automatically tune large systems of magnets and RF set points to optimize beam parameters [18], it has been utilized in hardware at the proton linear accelerator at the Los Alamos Neutron Science Center (LANSCE) to automatically tune two RF buncher cavities to maximize the RF system's beam acceptance, based only on a noisy measurement of beam current [19], and it has been utilized at the Facility for Advanced Accelerator Experimental Tests (FACET), to non-destructively predict electron bunch properties via a coupling of simulation and machine data [20].

The model independence of ES and its ability to op-

* ascheink@lanl.gov
† xiahuang@slac.stanford.edu

This material is based upon work supported by the U.S. Department of Energy, Office of Science, under Contract No. DE-AC02-76SF00515.

timize uncertain time-varying system, makes it ideal for performing automatic feedback for continuous re-tuning of many parameter systems in response to uncertain, time-varying disturbances. In this work we utilize ES for continuous re-tuning of the eight parameter system shown in Figure 1, in which the delay, pulse width, and voltage of two injection kickers, K_1 and K_2, as well as the current of two skew quadrupoles Q_1 and Q_2, were tuned in order to optimize the injection kicker bump match, minimizing betatron oscillations. In general, the coupled transverse motion of beams can be described as

$$x'' + k_x(s)x = f(x, y, s; t) \tag{1}$$
$$y'' + k_y(s)y = g(x, y, s; t) \tag{2}$$

where the sources of coupling functions $f(x, y, s; t)$ and $g(x, y, s; t)$ include misaligned magnets, magnetic field errors, solenoid fields, and skew components of magnetic field gradients, all of which may be time dependent due to the fluctuation of magnet power sources or diurnal thermal variations. In the case of injection kicks, the imperfect match of parameters (voltage, pulse width, etc...) of all of the magnets involved results in betatron oscillations. The main focus of this work was of automatically optimizing injection magnet matching, thereby decreasing the amplitude of betatron oscillations.

The experiment was performed on the SPEAR3 storage ring, a 3-GeV third-generation light source at SLAC National Accelerator Laboratory. The experimental setup for this work, of optimization by kicker bump matching, has been successfully tested via RCDS for a time-invariant system [13]. In this work, we demonstrate the ability of ES to optimize a many parameter, coupled, time-varying system, by purposely mismatching the injection kicker bump by continuously, quickly varying the magnetic field strength of the third kicker, $K_3(t)$, changing its power source voltage (and thereby it's magnetic field strength) $\pm 6\%$ via a sinusoidal trajectory over 1.5 hours. The ES feedback was able to continuously re-tune the four other magnets, maintaining minimal betatron oscillations, without knowledge of the voltage of the third kicker $K_3(t)$, based only on the measured variance of the electron beam's betatron oscillations over 256 turns.

II. ADAPTIVE TUNING ALGORITHM

The ES feedback scheme is designed for dynamic systems with many coupled parameters

$$\mathbf{p}(t) = (p_1(t), p_2(t), \ldots, p_m(t)), \tag{3}$$

with the goal of minimizing an analytically unknown, time-varying, user-defined "cost function," $C(\mathbf{p}, t)$, whose minimization corresponds to optimization of certain system properties (such as a beam loss monitor). The parameter adaptation takes place based on a possibly noise corrupted measurement of this function:

$$\hat{C}(\mathbf{p}, t) = C(\mathbf{p}, t) + \underbrace{\nu(t)}_{\text{noise}}. \tag{4}$$

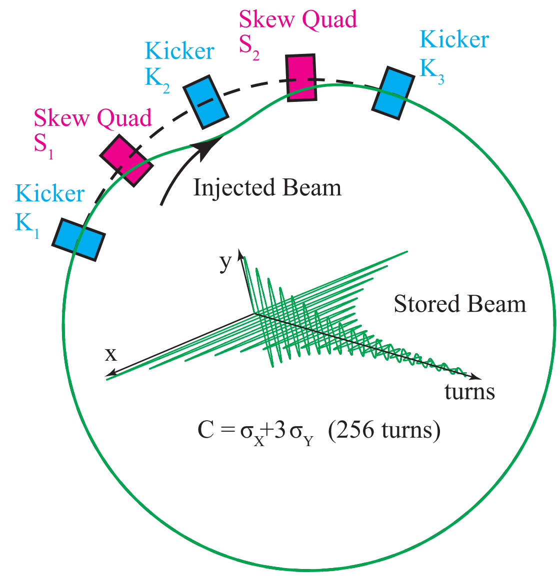

FIG. 1. Kicker magnets and skew quadrupole magnets.

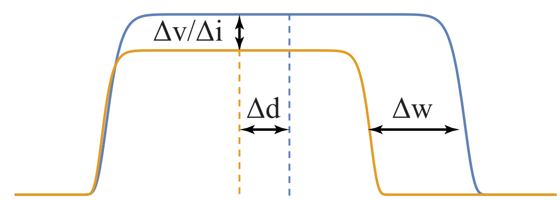

FIG. 2. Kicker magnet delay (d), pulse width (w), and voltage (v) were adaptively adjusted, as well as the skew quadrupole magnet currents (i).

All of the parameters are initialized with physics-based estimates of their optimal settings, $p_i(1)$. The discrete, iterative feedback parameter update law is then implemented as

$$\begin{aligned}
p_1(n+1) &= p_1(n) + \Delta\sqrt{\alpha\omega_1}\cos\left(\omega_1 \Delta n + k\hat{C}(n)\right) \\
p_2(n+1) &= p_2(n) + \Delta\sqrt{\alpha\omega_2}\cos\left(\omega_2 \Delta n + k\hat{C}(n)\right) \\
&\vdots \\
p_m(n+1) &= p_m(n) + \Delta\sqrt{\alpha\omega_m}\cos\left(\omega_m \Delta n + k\hat{C}(n)\right),
\end{aligned} \tag{5}$$

so that each new parameter setting is based only on the previous parameter setting and the previous, possibly noise-corrupted, cost function measurement

$$\hat{C}(n) = C(\mathbf{p}(n), t) + \nu(t). \tag{6}$$

The iterative scheme (5) is based on dynamic feedback

$$\frac{dp_i(t)}{dt} = \sqrt{\alpha\omega_i}\cos\left(\omega_i t + k\hat{C}(\mathbf{p}(t), t)\right), \quad \omega_i \neq \omega_j, \tag{7}$$

by utilizing the finite difference approximation

$$\frac{dp_i(t)}{dt} \approx \frac{p_i(t+\Delta) - p_i(t)}{\Delta}. \tag{8}$$

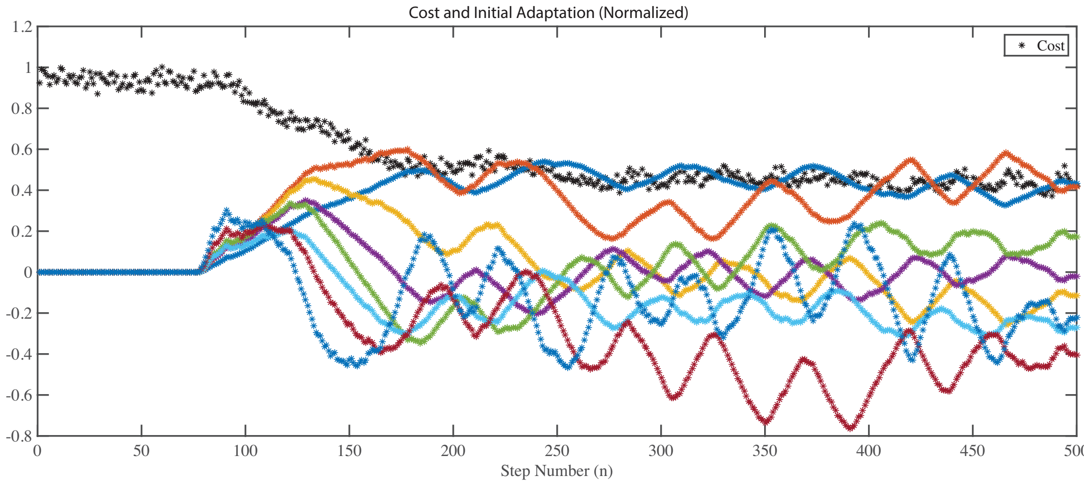

FIG. 3. The adaptive scheme is activated at around step 75, quickly minimizing the transverse beam oscillations by tuning 8 components simultaneously, with all values normalized within $[-1, 1]$. Within roughly 200 steps a minimum value has been reached. The black data points are the cost function evaluations and the colored data points, which all start at 0, show the amount of deviation of each component from its initial settings.

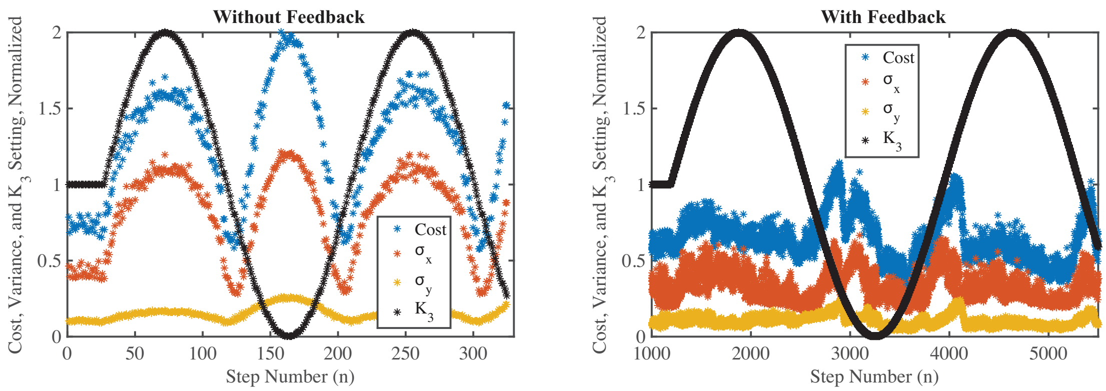

FIG. 4. **Left:** As the third kicker magnetic field, $K_3(t)$, is varied (black), the injector lattice becomes mis-matched, leading to large betatron oscillations, which are measured as the variance of the horizontal and vertical beam position monitor readings. **Right:** When ES is utilized, despite a time-varying $K_3(t)$, the remaining magnets are continuously re-tuned in order to maintain a good match and minimal betatron oscillations.

For large ω_i, (7) or (5) result in average parameter dynamics of the form

$$\frac{d\mathbf{p}(t)}{dt} = -\frac{k\alpha}{2}\nabla C^T(\mathbf{p}(t), t), \tag{9}$$

which is a gradient descent towards a minimizing value of $C(\mathbf{p}(t), t)$, which does not require analytic knowledge of the function C, and does not perform any kind of finite-difference gradient estimation which is especially problematic in noisy environments. Several important features of this feedback scheme are:

1. On average the gradient descent, (9), takes place relative to the actual, unknown function $C(\mathbf{p}(t), t)$, despite being based only on its noise-corrupted measurement $\hat{C}(n) = C(\mathbf{p}(n), t) + \nu(t)$.

2. Despite operating on an analytically unknown function, $\hat{C}$, this feedback has the nice (and safe) feature of having analytically known bounds on parameter variation and update rates, because the unknown function enters the parameter dynamics as the argument of a known, bounded function:

$$\begin{aligned} |p_i(n+1) - p_i(n)| &= \left|\Delta\sqrt{\alpha\omega_i}\cos\left(\omega_i\Delta n + k\hat{C}(n)\right)\right| \\ &= \left|\Delta\sqrt{\alpha\omega_i}\right|\left|\cos\left(\omega_i\Delta n + k\hat{C}(n)\right)\right| \\ &\le \left|\Delta\sqrt{\alpha\omega_i}\right|. \end{aligned} \tag{10}$$

Enforcing bounds on parameters is trivially accomplished by checking that each parameter is within prescribed bounds $p_{i,\min} < p_i(n+1) < p_{i,\max}$ before performing

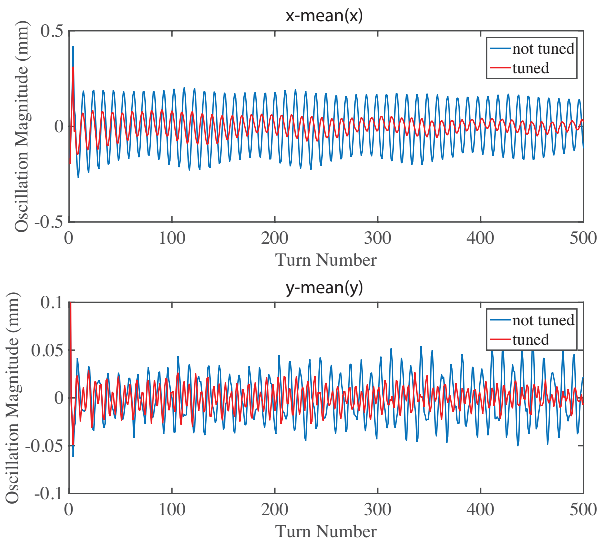

FIG. 5. BPM readings of x and y beam displacement over 500 turns, before and during tuning.

parameter updates. A more detailed mathematical background is available in [16–20].

A. Choosing the parameters k, α, ω_i, and Δ.

The parameter $k > 0$ acts as the feedback gain, with the velocity of the on-average gradient descent (9) being proportional to k. If gradient ascent is desirable (maximization instead of minimization), $k > 0$ may simply be replaced with $k < 0$.

The parameter $\alpha > 0$ also acts as a feedback gain, as it shows up in (9), but more importantly, as feedback takes place, the size of the dither of each parameter is proportional to $\sqrt{\alpha}$, as shown in (5) and (7). Therefore, increasing α may help one to escape local minima by introducing larger perturbations in parameter values.

Once α and k are chosen, the dithering frequencies, ω_i must be chosen to be distinct,

$$\omega_i = \omega r_i, \quad i \neq j \ \rightarrow \ r_i \neq r_j, \tag{11}$$

so that the perturbing functions are orthogonal in the frequency domain. Orthogonality in the frequency domain means the products of the functions uniformly converge to zero in the L^2 norm on compact sets of the form $[0, T]$, as ω is increased to infinity:

$$\lim_{\omega \rightarrow \infty} \int_0^T \cos(\omega r_1 t) \cos(\omega r_2 t) dt = 0. \tag{12}$$

The $\cos(\cdot)$ functions in (5), (7) may be replaced by $\sin(\cdot)$ functions or any orthogonal functions including triangle or square waves or mixtures of sines and cosines. The analytical result giving the average system (9) is based on an assumption that ω is chosen large enough so that it dominates any other time-varying components of the system. Therefore, in practice, first α and k are chosen and then ω is increased until the desired performance is achieved.

The term Δ must be chosen small enough relative to the ω_i so that the finite difference approximation (8) is reasonable and the various dithering frequencies are distinguishable. For example, a typical value of Δ may be $\Delta = \frac{2\pi}{20 \max\{\omega_i\}}$.

B. Implementation at SPEAR3

At SPEAR3, we simultaneously tuned 8 parameters:

- p_1: K_1 delay
- p_2: K_1 pulse width
- p_3: K_1 voltage
- p_4: K_2 delay
- p_5: K_2 pulse width
- p_6: K_2 voltage
- p_7: SQ_1 current
- p_8: SQ_2 current

which are illustrated in Figure 2. While controlling the voltage for the kicker magnets K_1, K_2, and the current for the skew quadrupole magnets SQ_1, SQ_2, in each case a change in the setting resulted in a change in magnetic field strength.

The cost used for tuning was a combination of the horizontal and vertical variance of beam position monitor readings over 256 turns, the minimization of which resulted in decreased betatron oscillations,

$$\begin{aligned} C(t, p(t)) &= \sigma_x + 3\sigma_y \\ &= \sqrt{\frac{1}{256}\sum_{i=1}^{256}(x(i) - \bar{x})^2} \\ &\quad + 3\sqrt{\frac{1}{256}\sum_{i=1}^{256}(y(i) - \bar{y})^2}, \end{aligned} \tag{13}$$

where the factor of 3 was added to increase the weight of the vertical oscillations, which require tighter control since the vertical beam size is much smaller and therefore users are more sensitive to vertical oscillations.

III. EXPERIMENTAL RESULTS

A. Tuning of a time-invariant system

We started by demonstrating the ability to tune the 8 parameter system without adding artificial time-varying

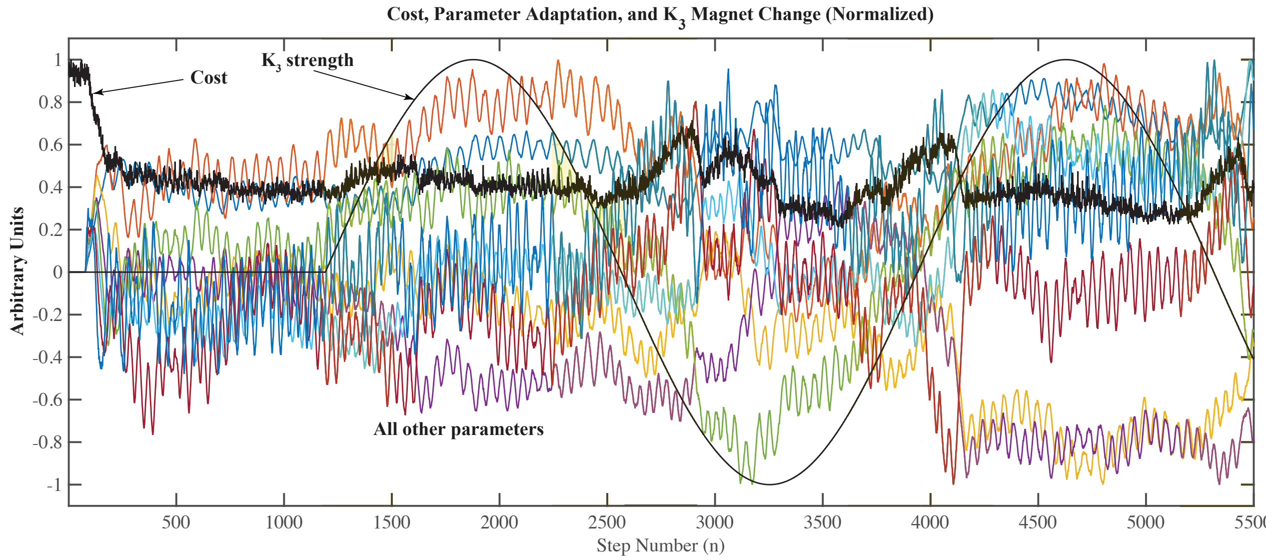

FIG. 6. Evolution of the cost, adaptively tuned magnet settings, and time-varying $K_3(t)$ magnet field, all normalized to within $[-1, 1]$. Initially, the cost quickly settles to a minimum value. Once the magnetic field strength of the third kicker magnet, K_3, begins to vary, the adaptive scheme re-tunes all parameters in real time to maintain a low cost and therefore low oscillations. The cost has visible bumps at those places where the rate of change of K_3 is highest (yellow highlighted regions). Such bumps can be further reduced by increasing the controller gains k, α, and perturbing frequency ω.

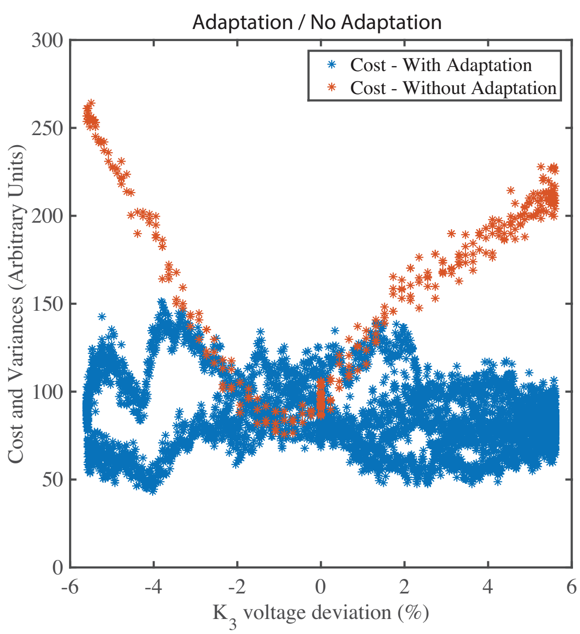

FIG. 7. Comparison of beam quality with and without adaptation.

perturbations. The ES scheme was implemented by setting parameter values, kicking an electron beam out and back into the ring, and recording beam position monitor data for 256 turns. Based on this data the cost was calculated as in (13), based on a measurement of the horizontal and vertical variance of beam position monitor readings. Minimization of the cost resulted in better matched magnet settings and smaller residual betatron oscillations. The results are shown in Figure 3, where ES is turned on at step 75 and the cost is quickly minimized within ~ 150 steps of the algorithm, after which the parameters continued to oscillate about their steady state values. In order to prevent persistent parameter oscillation, a dead zone based on desired performance may easily be implemented, so that the feedback turns on only when system performance drifts out of some pre-determined bounds.

B. Tuning of a time-varying system

In the second experiment, to demonstrate the scheme's ability to compensate for an uncertain, time-varying perturbation of the system, we purposely varied the voltage (and therefore resulting magnetic field strength) of the third kicker magnet, $K_3(t)$. The kicker voltage was varied sinusoidally over a range of $\pm 6\%$ over the course of 1.5 hours, which is a very dramatic and fast change relative to actual machine parameter drift rates and magnitudes.

The left side of Figure 4 shows the influence that varying the magnetic field strength, $K_3(t)$, has on the variance of the vertical and horizontal beam position monitor readings as the kicker settings, and therefore, from the point of view of the beam, the injection lattice is repeatedly brought in and out of match. The right side of Figure 4 shows the result when the feedback ES scheme is activated. Despite a quickly time varying $K_3(t)$, the ES is able to continuously re-tune the other kicker and lattice parameters to maintain a good match. Figure 5 shows a typical beam position monitor reading without and with ES tuning, during variation of $K_3(t)$, over 500 turns. Figure 6 shows the evolution of all parameters, cost, and $K_3(t)$ over 1.5 hours. Finally, Figure 7 shows the cost, which is a function of betatron oscillation, versus magnet setting $K_3(t)$, with and without ES feedback. For large magnetic field deviations, the improvement is roughly a factor of 2.5.

IV. CONCLUSIONS AND FUTURE WORK

In this work we have demonstrated, in hardware, a very simple model-independent feedback scheme for the tuning of many coupled parameters for the optimization of an uncertain, time-varying system. We believe that this scheme can be useful for any complex, noisy, time-varying system which typically requires operator-based re-tuning by hand or for systems for which accurate, real-time analytic models do not exist or are prohibitively computationally expensive.

V. ACKNOWLEDGEMENTS

The kicker bump matching setup for SPEAR3 was originally developed by James Safranek and used in [13]. The study was supported by DOE Contract No. DE-AC02-76SF00515 (SLAC), US DOE Office of Science Early Career Research Program grant FWP-2013-SLAC-100164, and Los Alamos National Laboratory.

[1] M. Borland, Report No. APS LS-287 (2000).
[2] R. Hajima, N. Taked, H. Ohashi, and M. Akiyama, "Optimization of wiggler magnets ordering using a genetic algorithm," Nucl. Instrum. Methods Phys. Res., Sect. A 318, 822 (1992).
[3] I. Bazarov and C. Sinclair, "Multivariate optimization of a high brightness dc gun photo injector," Phys. Rev. ST Accel. Beams 8, 034202 (2005).
[4] L. Emery, in Proceedings of the 21st Particle Accelerator Conference, Knoxville, 2005 (IEEE, Piscataway, NJ, 2005).
[5] M. Borland, V. Sajaev, L. Emery, and A. Xiao, in Proceedings of the 23rd Particle Accelerator Conference, Vancouver, Canada, 2009 (IEEE, Piscataway, NJ, 2009).
[6] L. Yang, D. Robin, F. Sannibale, C. Steier, and W. Wan, "Global optimization of an accelerator lattice using multiobjective genetic algorithms," Nucl. Instrum. Methods Phys. Res., Sect. A 609, 50 (2009).
[7] A. Poklonskiy and D. Neuffer, "Evolutionary algorithm for the neutrino factory front end design," Int. J. Mod. Phys. A 24, 5 (2009).
[8] W. Gao, L. Wang, and W. Li, "Simultaneous optimization of beam emittance and dynamic aperture for electron storage ring using genetic algorithm," Phys. Rev. ST Accel. Beams 14, 094001 (2011).
[9] R. Bartolini, M. Apollonio, and I. P. S. Martin, "Multiobjective genetic algorithm optimization of the beam dynamics in linac drivers for free electron lasers," Phys. Rev. ST Accel. Beams 15, 030701 (2012).
[10] A. Hofler, B. Terzic, M. Kramer, A. Zvezdin, V. Morozov, Y. Roblin, F. Lin, and C. Jarvis, "Innovative applications of genetic algorithms to problems in accelerator physics," Phys. Rev. ST Accel. Beams 16, 010101 (2013).
[11] X. Huang and J. Safranek, "Nonlinear dynamics optimization with particle swarm and genetic algorithms for SEPAR3 emittance upgrade," Nucl. Instrum. Methods Phys. Res., Sect. A 757, pp. 48-53, 2014.
[12] K. Tian, J. Safranek, and Y. Yan, "Machine based optimization using genetic algorithms in a storage ring," Phys. Rev. Accel. Beams 17, 020703, 2014.
[13] X. Huang, J. Corbett, J. Safranek, and J. Wu, "An algorithm for online optimization of accelerators," Nuclear Instruments and Methods in Physics Research A, vol. 726, pp. 77-83, 2013.
[14] H. Ji, S. Wang, Y. Jiao, D. Ji, C. Yu, Y. Zhang, X. Huang, "Discussion on the problems of the online optimization of the luminosity of BEPCII with the robust conjugate direction search method," in Proceedings of the International Particle Accelerator Conference, Shanghai, China, 2015.
[15] X. Huang and J. Safranek, "Online optimization of storage ring nonlinear beam dynamics," Phys. Rev. ST Accel. Beams 18.8, 084001, 2015.
[16] A. Scheinker, M. Krstic, "Minimum-seeking for CLFs: Universal semiglobally stabilizing feedback under unknown control directions," *IEEE Transactions on Automatic Control*, vol. 58, pp. 1107-1122, 2013.
[17] A. Scheinker, M. Krstic, 'Extremum seeking with bounded update rates," *Systems & Control Letters*, vol. 63, pp. 25-31, 2014.
[18] A. Scheinker, X. Pang, L. Rybarcyk, "Model-independent particle accelerator tuning," *Physical Review Special Topics - Accelerators and Beams*, vol. 16.10, 102803, 2013.
[19] A. Scheinker, S. Baily, D. Young, J. Kolski, M. Prokop, "In-hardware demonstration of model-independent adaptive tuning of noisy systems with arbitrary phase drift," Nucl. Instrum. Methods Phys. Res., Sect. A, 756, (2014) 30-38.
[20] A. Scheinker and S. Gessner , "Adaptive method for electron bunch profile prediction," *Physical Review Special Topics - Accelerators and Beams*, vol. 18.10, 102801, 2015.